Hybrid Advances 11 (2025) 100549

Contents lists available at ScienceDirect

Hybrid Advances

journal homepage: www.journals.elsevier.com/hybrid-advances

Research Article

Utilization of poly-2-hydroxypropane-1,2,3-tricarboxylic carubin as a glidant in lactose granules

Wuryanto Hadinugroho *, Stephanie Florencia Winarko, Echa Imanuela Sinta, Senny Yesery Esar, Jefri Prasetyo

Faculty of Pharmacy, Widya Mandala Surabaya Catholic University, Kalisari Selatan No. 1. Pakuwon City, Surabaya, 60112, Indonesia

ARTICLE INFO

Keywords:
Carubin
2-Hydroxypropane-1,2,3-tricarboxylic acid
P-2HTCb
Lactose granul
Glidant

ABSTRACT

Poly-2-hydroxypropane-1,2,3-tricarboxylic carubin (P-2HTCb) has characteristics as a glidant similar to talc and magnesium stearate (MgSt), such as irregular shape, wavy surface, difficulty dissolving in water, and hydrophobicity. The experiment's purpose is to determine the effect and potential of P-2HTCb as a glidant in tablet dosage form with lactose granules (LG) as a filler model. The application of P-2HTCb as a glidant represents a novelty. P-2HTCb was used in each of mixture mass with contents of 0.5 %, 1 %, 2 %, and 4 %. Each mixture mass was tested for flow time, angle of repose, and Tap-Bulk, then tableted with a weight of 700 mg. The tablets were tested for hardness, friability, and disintegration time. Evaluation of the mixture mass with concentrations of 0.5 %, 1 %, 2 %, and 4 % for flow time 5.13–5.47 s; angle of repose 21.54–22.56°; Tap-Bulk 0.070–0.078 g mL^{-1}; tablet weight 699.7–702.0 mg; tablet hardness 7.9–8.4 kp; Tablet friability 0.70–0.86 % and tablet disintegration time 0.52–1.63 min. The optimum concentration (2 %) improves the flow time and angle of repose of the mixture mass. Increasing the concentration of P-2HTCb causes the Tap-Bulk value of the mixture mass and tablet friability to decrease, but increases tablet hardness. The optimum concentration (1 %) provides the fastest disintegration time. P-2HTCb produces minimal dust when mixed with LG material. P-2HTCb can be recommended as an alternative glidant candidate in environmentally and health-friendly pharmaceutical formulations.

1. Introduction

2-hydroxypropane-1,2,3-tricarboxylic acid (2HT) reacts with carubin (Cb) under acidic conditions to form an ester polymer, poly-2-hydroxypropane-1,2,3-tricarboxylic carubin (P-2HTCb) [1,2]. The specific characteristics of P-2HTCb align with those of typical esterification products, including ester carbonyl groups, low solubility, and low viscosity. Characteristics derived from galactomannan that may appear in P-2HTCb include amorf, irregular particle shape, and a wavy surface [2,3].

Glidant is a fine powder that coats particles, smoothing their surfaces and improving flow. It also fills the pores of filler granules, resulting in smoother surfaces and enhanced flowability [4]. Talc and magnesium stearate (MgSt) are commonly used glidants in the pharmaceutical industry due to their availability and low cost. Both have fine particle size, are hydrophobic, water-insoluble, and exhibit irregular shapes with wavy surfaces [5–7]. P-2HTCb shares similar characteristics with talc and MgSt, warranting evaluation of its glidant potential. Talc contains inorganic silicates that can slightly absorb humidity [8,9]. MgSt is an organic compound derived from saturated fatty acid stearate, functioning as a envelop that renders particle surfaces slippery [10–12]. P-2HTCb is an ester of mannose-galactose and 2-hydroxypropane-1,2,3-tricarboxylic acid. Organoleptic tests indicate that P-2HTCb exhibits waxy properties.

This study aims to evaluate the effect and potential of P-2HTCb as a glidant in tablet formulations, using lactose granules (LG) as a filler model. P-2HTCb was used at concentrations of 0.5 %, 1 %, 2 %, and 4 %, similar to those applied for talc and MgSt as controls. These concentrations reflect typical usage levels of talc (1.00–10.00 %) and MgSt (0.25–5.00 %) in solid dosage formulations to facilitate particle flow [13,14]. Each formulation was tested for flow time, angle of repose, and Tap-Bulk, then compressed into 700 mg tablets. The tablets were evaluated for hardness, friability, and disintegration time. LG was prepared from a lactose monohydrate solution by rapid wetting and spraying to form spherical agglomerates. It is commonly used as a filler in direct compression. LG characteristics include spherical or granular shape,

* Corresponding author.
E-mail address: wuryanto.hadinugroho@ukwms.ac.id (W. Hadinugroho).

https://doi.org/10.1016/j.hybadv.2025.100549
Received 25 July 2025; Received in revised form 8 September 2025; Accepted 16 September 2025
Available online 16 September 2025

porosity, water solubility, and hydrophilicity [6].

The application of P-2HTCb as a glidant represents a novelty. This study investigates the influence of increasing P-2HTCb concentrations on the flowability of the mixture mass and the quality of tablets to conventional glidants such as talc and MgSt. Both comparators generated visible dust during mixing due to their low bulk densities, approximately 0.56 g cm^{-3} for talc and 0.16 g cm^{-3} for MgSt [6,15]. In contrast, P-2HTCb, synthesized from carubin (Cb) and 2-hydroxypropane-1,2,3-tricarboxylic acid (2HT), is estimated to possess a higher bulk density, given the densities of its precursors (0.63 g cm^{-3} for Cb and 0.60 g cm^{-3} for 2HT) [16–18]. This property suggests a potential reduction in dust formation during mixing. P-2HTCb was tested at concentrations ranging from 0.5 % to 4.0 % to assess potential as glidant. The results provide insight into its potential as an alternative glidant for solid dosage formulations.

2. Material and methods

Standard materials, chemicals, and equipment commonly used in manufacturing and evaluation in the food and pharmaceutical fields were used to obtain quality P-2HTCb, quality tablets, and glidant potential determination. Chemical characterization such as UATR and NMR to ensure the success of P-2HTCb manufacturing, while physical characterization such as viscosity, pH, and solubility to ensure new properties that emerge from P-2HTCb. Manufacturing of mixed mass and tablets was carried out using research-scale production tools. Evaluation of the quality of mixed mass and tablets such as flow time, angle of repose, Tap-Bulk, tablet weight, hardness, friability, and disintegration time followed standard reference procedures.

2.1. Raw materials and chemicals

The experimental ingredients were carubin (food grade, Viscogum, Cargill, France), 2-hydroxypropane-1,2,3-tricarboxylic acid (pro analytical, Merk KgaA, Darmstadt, Germany), hydrochloric acid (pro analytical, Sigma Aldrich Chemie, GmbH, USA), water for injection (sterile grade, PT. Otsuka Indonesia), aquadest (technical grade, Cawan Anugerah Chemika, Indonesia), acetone t.g (Cawan Anugerah Chemika, Indonesia), lactose granules (pharmaceutical grade, FlowLac 90, Meggle GmbH & Co. KG, Germany), talc (food grade, PT. Bratachem, Indonesia) and magnesium stearate (food grade, PT. Bratachem, Indonesia).

2.2. Manufacturing of P-2HTCb

P-2HTCb was created by adopting previous research methods [19]. Cb (7.10 x 10^{-6} mol) was swollen in water for injection (up to 50 mL), adding 0.42 mol of 2HT and 0.24 mol of HCl (acid catalyst). The gel mixture was heated at 50 °C in a water bath for 30 min (Fig. 1). The gel was precipitated with acetone and repeatedly rinsed with acetone-aquadest (1:1). The P-2HTCb slabs were dried and powdered by a blender (Maspion, MT1569). P-2HTCb powder was analyzed using Fourier Transform Infrared (FTIR), Nuclear Magnetic Resonance (NMR), viscosity, and pH.

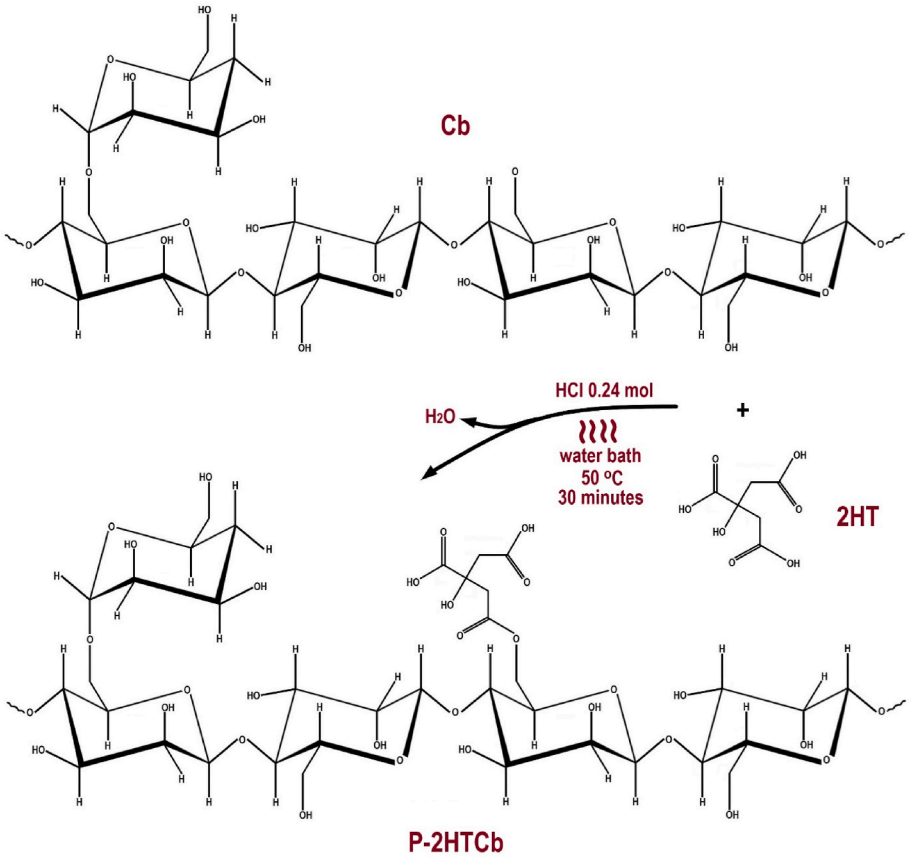

Fig. 1. P-HTCb manufacturing mechanism. The mechanism begins with the protonation of the O atom in the 2HT carbonyl group. The O atom attacks H^+ in HCl to create ^+OH. The C–OH of mannose and galactose attacks the C atom in the 2HT carbonyl group, causing the release of the double bond in the C═O group, thus creating $(OH)_2$ and CO^+ -H groups. Proton transfer occurs from CO^+-H to the OH group, creating H_2O^+ and CO in mannose and galactose. The H^+ in the OH group is lost, followed by H_2O^+, which is called H_3O^+. The mechanism concludes that the C atom in mannose and galactose replaces the H atom from 2HT in the carboxylate group.

2.3. Characterization of P-2HTCb

P-2HTCb powder was infrared analyzed with UATR (PerkinElmer Spectrum Version 10.4.3., USA). Analysis was carried out at wave numbers 400-4000 cm^{-1}. P-2HTCb was analyzed with ^{1}H and ^{13}C NMR (JEOL RESONANCE ECZ 500R, Japan). The viscosity of P-2HTCb was analyzed with a viscometer (Brookfield LVDV-I Prime, AP6510416, USA) using an S61 spindle at 60 rpm. The acidity of P-2HTCb was analyzed with a pH meter (Metrohm 913, Switzerland), which had been calibrated at pH 4, 7, and 10. The 0.5 g of P-2HTCb was dispersed in 50 mL of distilled water and stirred using a magnetic stirrer for 2× 12 h (OHAUS Guardian 3000, USA). The resulting mixture was filtered, and the filtrate was dried in a 70 °C water bath and then weighed (Mettler Toledo AL204, Switzerland). Solubility was calculated as the percentage ratio of the dried filtrate weight to the initial sample weight [2].

2.4. Preparation of mixture mass and tablet

P-2HTCb and the two comparators (talc and MgSt) were weighed following the research design (Table 1) for concentrations of 0.5 %, 1 %, 2 %, and 4 %. The LG was weighed up to 100 g of the mixture mass. Each mixture mass was mixed until homogeneous on a cubic mixer (50 rpm, 1 min) (Erweka, Germany). Each mixture mass was compressed into 700 mg tablets using a single punch tablet press on a scale of 10–12 (max. pressure 3.000 kg/cm^2) by direct compression (Bio/Pharmatech, R&D Press, Taiwan). The tablets were evaluated for hardness, friability, and disintegration time.

2.5. Flowability

Each mixture mass (100 g) was poured into the funnel of a flowability tester (Erweka, Germany). The start button is pressed to open the funnel valve so the mixture mass flows towards the sample plate. The flow time for 100 g is displayed on the monitor. The cone-shaped mound on the plate is scanned using infrared to determine its dimensions. The angle of repose is displayed on the monitor.

2.6. Tap-Bulk

The graduated cylinder (100 mL) was carefully weighed on an digital balance (Mettler Toledo, Switzerland), and the weight was recorded. The mixture mass was poured slowly into a measuring cup at a slope of approximately 45° until 100 mL was reached. The measuring cup containing the powder was weighed again, and the weight was recorded. The measuring cup was placed on a tap density volumeter (Erweka, Germany). The start button was pressed to tap 500 times. Observe and note the volume at the end of the beat. The actual weight of the mixture mass was obtained from the difference between the glass containing the mixture mass and the empty measuring cup (*w*). Bulk density was obtained from the powder weight and initial volume (100 mL) ratio. Tap density was obtained from the powder weight and final tapping volume ratio. Tap-Bulk was obtained following Equation (1) [20].

$$\text{Tap} - \text{Bulk} = \left[\frac{W}{v'}\right] - \left[\frac{W}{v}\right] \quad (1)$$

w is the mass weight of the mixture mass, v' is the volume of the mixture mass final tapping, and v is the volume of the mixture mass before tapping.

Table 1
Experimental formulas with various types and concentrations of glidants.

Material	Glidant concentration [%]			
P-2HTCb/talc/MgSt	0.5	1	2	4
LG ad [g]	100	100	100	100

2.7. Tablet weight

Several tablets (20 units) were taken randomly, and the weight was determined by weighing them individually (Mettler Toledo, Switzerland). The average weight and standard deviation of each batch were determined.

2.8. Hardness

Representative tablets of 6 units from each batch were taken randomly. Each tablet was pressed by a metal rod until it cracked or broke on a hardness testing apparatus (Schleuniger, Netherlands). The hardness of each tablet is measured by the pressure in kg pounds (kp) displayed on the monitor [21,22].

2.9. Friability

Representative tablets of 10 units from each batch were taken randomly. All tablets were dusted free and weighed. They were then placed in a drum friability apparatus (Erweka, Germany) and rotated at 25 rpm for 4 min. All tablets were dusted again and weighed. Friability was determined according to Equation (2) [20–22].

$$\text{Friability } [\%] = \left[\frac{\text{initial weight} - \text{final weight}}{\text{initial weight}}\right] \text{x } 100\% \quad (2)$$

2.10. Disintegration time

Representative tablets of 18 units from each batch were randomly selected. Six tablets out of 18 were randomly selected. Each tube in the apparatus disintegration vessel (Erweka Z3, Germany) was filled with tablets. The vessel was repeatedly raised and lowered to be immersed in distilled water (900 mL, 37 °C) in the chamber [23]. The longest time for the six tablets to leave the tube was the disintegration time [20].

2.11. Statistics

Two-factor ANOVA was used for flow time, angle of repose, Tap-Bulk, hardness, friability, and disintegration time tests. Glidant type and experimental concentration were factors for ANOVA with alpha (α) 0.05.

3. Result and discussion

Experimental data are presented systematically to facilitate interpretation of the results of P-2HTCb characterization, blended mass quality evaluation, and tablet quality evaluation. This process serves as a method for determining the glidant potential of P-2HTCb, considering the influence and advantages of P-2HTCb on tablet formulation and manufacturing technology.

3.1. Manufacturing of P-2HTCb

P-2HTCb manufacturing was tailored to laboratory-scale capacity and facilities and followed previous research methods [2] The average yield of dry P-2HTCb was 1.20 g ± 0.06. All P-2HTCb was mixed and pureed with a blender. P-2HTCb fine powder was characterized before being used for P-2HTCb research as a glidant.

3.2. Characterization of P-2HTCb

The infrared spectrum of P-2HTCb is shown in Fig. 2. P-2HTCb identified the O–H group as appearing at 3337.44 cm^{-1}, C–H as 2923.86 cm^{-1} and 2851.60 cm^{-1}, and C═O ester as 1735.84 cm^{-1}. The spectrum of P-2HTCb is similar to that of Cb, except that the C═O ester group is present in P-2HTCb. The C═O ester group is a specific group that

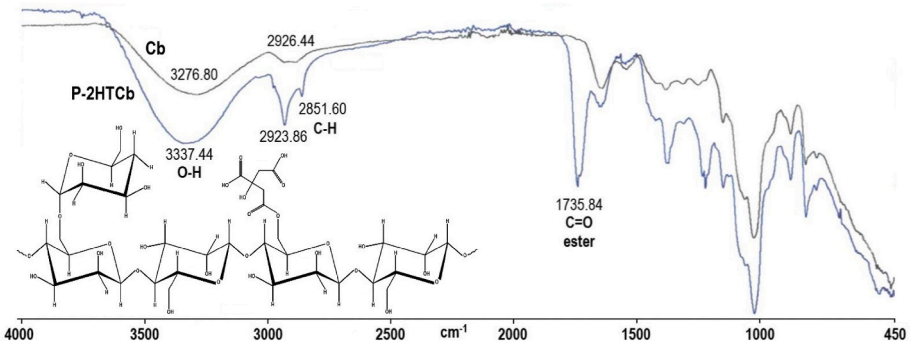

Fig. 2. Infrared spectra of P-2HTCb and Cb. The specific group of P-2HTCb is the C═O ester group, which appears at wave number 1735.84 cm^{-1}.

identifies successful esterification. Wave numbers in previous research showed the O–H group was around 3300 cm^{-1}, C–H around 2800 and 2900 cm^{-1}, and C═O ester around 1735-1740 cm^{-1} [1,3]. The NMR spectrum of P-2HTCb is shown in Fig. 3. ^{1}H NMR of P-2HTCb shows two doublet peaks at $\delta = 3.047$ ppm and $\delta = 3.015$ ppm (E,F), $\delta = 2.866$ and ppm, and $\delta = 2.834$ ppm (E,F) which corresponds to C–H_2 (symmetric side) from 2HT. Both twin peaks indicate the presence of 2HT in Cb. The other protons of mannose and galactose are close, so peaks coincide. Multiple peaks at $\delta = 4.114$–3.427 ppm correspond to C–H of C s in mannose and galactose. Details of multiple peak mannose and galactose peaks include $\delta = 4.114$ ppm (M2), $\delta = 3.750$ ppm (M3), $\delta = 3.895$ ppm (M4), $\delta = 3.551$ ppm (M5), $\delta = 3.736$ ppm (M6), $\delta = 3.803$ ppm (G2), $\delta = 3.920$ ppm (G3), $\delta = 3.979$ ppm (G4), $\delta = 3.775$ ppm (G5), and $\delta = 3.728$ ppm (G6). Previous experiments showed two doublet peaks from 2HT at $\delta = 3.083$–2.714 ppm [2,3]. Multiple peaks of mannose and galactose appear at $\delta = 4.418$–3.309 ppm [2,3]. ^{13}C NMR of P-2HTCb appears to peak at $\delta = 177{,}058$ ppm and $\delta = 173{,}593$ ppm corresponds to C═O of 2HT (A,B). The peak at $\delta = 73{,}383$ ppm corresponds to the central C of 2HT (C). The peak at $\delta = 43{,}358$ ppm corresponds to the C–H_2 symmetric side of 2HT (D). The peaks $\delta = 100{,}154$ ppm, $\delta = 76{,}541$ ppm, and $\delta = 75{,}034$ ppm correspond to C in the cyclohexane of mannose (M). The peaks at $\delta = 71{,}415$ ppm, $\delta = 69{,}937$ ppm, $\delta = 69{,}303$ ppm, $\delta = 61{,}240$ ppm, $\delta = 60{,}981$ ppm, and $\delta = 60{,}521$ ppm correspond to C in cyclohexane of mannose and galactose (M & G). The peaks do not appear well separated because P-2HTCb swells when wetted with deuterium (D_2O) as a medium for NMR analysis. Previous research reported that the peak at $\delta = 180$–170 ppm indicates the C═O group. The peak at $\delta =$ 80-70 ppm indicated the central C atom. The peak at $\delta = 44$-43 ppm indicated C–H and C–H_2 [1,24,25]. The peak at $\delta = 105$-60 ppm indicates mannose and galactose [2,26–29]. The viscosity of P-2HTCb in this study was 9.53 cP ± 0.15. The viscosity of P-2HTCb in previous studies was 7.82–11.37 cP [1–3]. The pH of P-2HTCb in this study was 4.83. The pH of 2HT used in this study was 2.05, and the pH of Cb was 5.85. The pH of P-2HTCb (4.83) shows the presence of 2HT in Cb, so the pH of P-2HTCb is between the pH of 2HT and Cb. The solubility of P-2HTCb in this experiment was 0.30 % ± 0.02. The P-2HTCb has been characterized and used in P-2HTCb research as a glidant in LG fillers.

3.3. Flow time

Table 2 and Fig. 4a show this study's flow time values. According to pharmaceuticals, a good mixture or powder mass flow time is ≤ 10 s for 100 g of mixture mass or powder [30–33]. The P-2HTCb mixture mass

Table 2
Evaluation values of mixture mass for flow time, angle of repose, and Tap-Bulk.

Glidant	Concentration [%]	Flow time [sec.]	Angle of repose [°]	Tap-Bulk [g.mL^{-1}]
Talc	**0.5**	6.40 ± 0.20	22.77 ± 0.21	0.066 ± 0.007
	1.0	6.73 ± 0.23	25.22 ± 0.26	0.080 ± 0.008
	2.0	6.80 ± 0.20	24.60 ± 0.26	0.072 ± 0.007
	4.0	7.00 ± 0.20	23.58 ± 0.31	0.066 ± 0.007
MgSt	**0.5**	6.20 ± 0.20	22.81 ± 0.25	0.047 ± 0.004
	1.0	5.20 ± 0.20	21.91 ± 0.27	0.054 ± 0.004
	2.0	5.87 ± 0.12	22.69 ± 0.24	0.076 ± 0.008
	4.0	8.67 ± 0.31	24.17 ± 0.24	0.094 ± 0.008
P-2HTCb	**0.5**	5.40 ± 0.20	22.56 ± 0.22	0.078 ± 0.004
	1.0	5.33 ± 0.23	22.00 ± 0.20	0.076 ± 0.004
	2.0	5.13 ± 0.31	21.54 ± 0.21	0.072 ± 0.004
	4.0	5.47 ± 0.12	22.42 ± 0.21	0.070 ± 0.004

Flow time and angle of repose indicate that the mixture mass containing P-2HTCb glidant has slightly faster flow properties than the mixture mass containing the other two glidants. Tap-Bulk indicates that the mixture mass containing P-2HTCb has greater and/or greater interparticle porosity than the mixture mass containing the other two glidants.

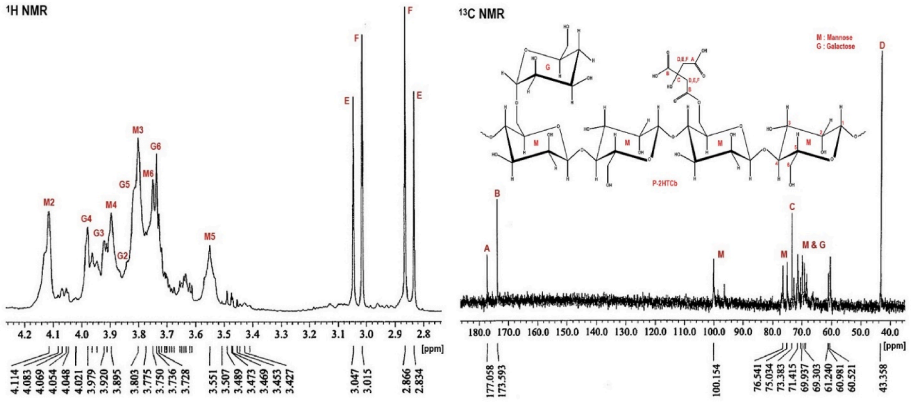

Fig. 3. ^{1}H and ^{13}C NMR spectra of P-2HTCb. The specific group P-2HTCb (C═O ester) appears at 177.058 ppm (central C atom) and 173.593 ppm (side C atom).

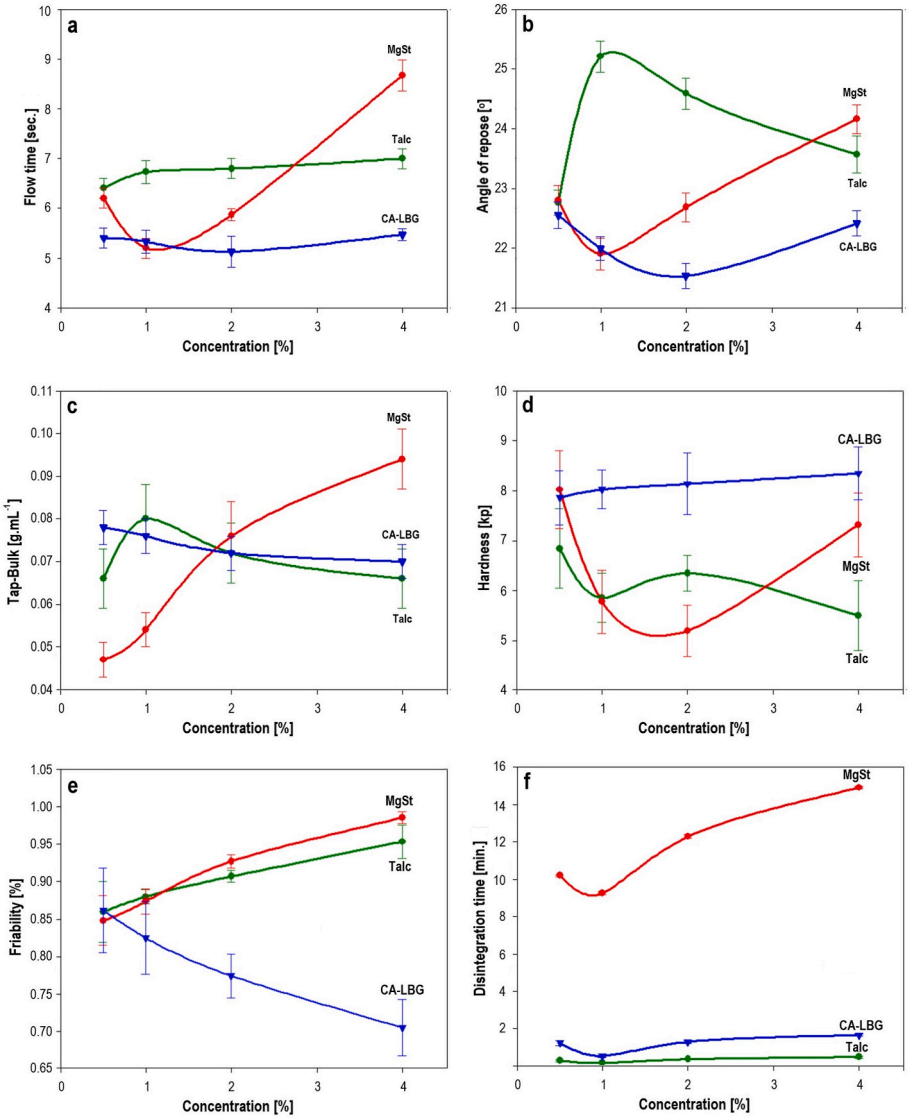

Fig. 4. Curve profile of glidant for flow time (a), angle of repose (b), Tap-Bulk (c), hardness (d), friability (e), and disintegration time (f). F_{count} from ANOVA for the effect of glidant type on flow time (65.6111), angle of repose (10.5786), Tap-Bulk (79.0034), hardness (79.0034), friability (1.2014), and disintegration time (1640.4846). F_{count} from ANOVA for the effect of glidant concentration on flow time (143.3571), angle of repose (177.2467), Tap-Bulk (3.1287), hardness (461.7071), friability (57.7262), and disintegration time (84150.9414). The criteria used for ANOVA are the effect of glidant type $F_{criteria}$ (3.0088) and the effect of glidant concentration $F_{criteria}$ (3.4028).

had the fastest flow time profile compared to the talc and MgSt mixture mass. The waxy properties of the P-2HTCb particles on the LG surface accelerate the LG movement in response to gravity so that the mixture mass flows quickly. P-2HTCb particles move freely between the LG surfaces along with the movement of the mixture mass, pushing the LG to move faster. The presence of talc on the LG surface and the porosity of the LG keep the LG in a dry condition because talc prevents humidity from penetrating the LG. A dry mixture mass will flow easily when exposed to gravity. A low concentration of MgSt particles on the LG surface can accelerate the mixture mass flow when exposed to gravity. The concentration increase of MgSt slows the mixture mass flow. The effect of stearate compounds as saturated fatty acids at low concentrations envelops the LG surface. In contrast, stearate compounds from MgSt at high concentrations cause cohesion between MgSt particles at the between LG's surface, thus inhibiting the flow of the mixture mass.

The number of P-2HTCb particles is sufficient to fill the porosity of the LG so that the particle surface is flat and flows easily. The higher the P-2HTCb concentration of 0.5 %–2 %, the faster the flow time. The 4 % concentration has a longer flow time than the three initial concentrations. P-2HTCb at the three concentrations filling the LG particles' porosity. In the P-2HTCb 4 %, the particles exceed the amount of LG porosity. The P-2HTCb particles in the form of fines inhibit the flow of the mixture mass.

The mixture mass of the talc shows that the higher the talc concentration, the slower the flow time. The number of talc particles exceeds the amount of LG porosity, so many talc particles are on the surface of the LG particles. The higher the talc concentration, the more cohesive layers of talc there are on the surface of the LG particles, thus inhibiting the movement of the LG particles.

The mixture mass of MgSt with a concentration of 0.5 % and 1 % could fastest the flow time because MgSt particles filled the porosity of the LG particles. The mass concentration mixture of 2 % and 4 % slows the flow time because more particles are on the surface of the LG, and more MgSt cohesive layers are formed. The flow time at both concentrations is longer than the mixture mass of the talc at the same concentration because the bulk density of MgSt (0.16 g cm^{-3}) is lower than that of talc (0.56 g cm^{-3}) [6,15]. Low density causes the powder volume to increase.

3.4. Angle of repose

Table 2 and Fig. 4b show the angle of repose values. A good angle of repose for a mixed mass or powder is $\leq 40^{\circ}$ [34,35]. The P-2HTCb mixture mass has the lowest angle of repose profile compared to the talc and MgSt mixture mass. The angle of repose results are in accordance with the flow time results. The presence of P-2HTCb particles that have waxy properties on the LG surface accelerates the movement of the mixture mass. LG at the top of the sharp cone moves freely continuously because the P-2HTCb particles also move freely between the LG surfaces, thus reducing the angle of repose of the mixture mass. Talc prevents the humidity of the mixture mass cone, but the movement of the mixture mass slows down because there is no driving force, thus tending to increase the angle of repose. The mixture mass cone containing low concentrations of MgSt accelerates the movement of LG. Rising concentrations of MgSt particles slow down the movement of the mixture mass. Stearic compounds derived from saturated fatty acids at low concentrations envelop the LG surface, thereby accelerating the movement of the mixture mass. At high concentrations, the MgSt stearate compound causes cohesiveness between MgSt particles on the LG's surface, thus inhibiting LG movement and increasing the angle of repose of the mixture mass.

A mixture with the number of P-2HTCb particles at a concentration of 0.5 %–2 % shows that the greater the porosity of the LG particles, the more they are filled with P-2HTCb particles. The surface of the LG particles becomes flatter and smoother as the concentration of P-2HTCb increases. The LG particles quickly move and flow above them, so that the mixture mass forms a cone that is not high and has a wide diameter. A mixture mass like this can easily fill the die space according to the designed weight. At a concentration of 4 %, the mixture mass shows that the number of P-2HTCb particles exceeds the porosity capacity, so these particles are located on the surface of the LG particles. Fine-sized P-2HTCb particles are difficult to flow and inhibit the movement of particles above them. In conditions like this, P-2HTCb particles can be arranged into several layers as the P-2HTCb concentration increases.

The angle of repose of the mass of the talc mixture with a concentration of 0.5 % did not show glidant activity because the number of particles was still too small to fill the porosity of the LG particles. The particles are few in the mixture mass with a concentration of 1 % on the surface of the LG particles, so the fines of talc particles inhibit the movement and flow of the particles above them. At concentrations of 2 %–4 %, the number of talc particles was able to fill the porosity and was on the surface of the LG particles. The surface of the LG particles becomes flat and smooth, thus facilitating the movement and flow of the particles above them.

The mixture mass of the MgSt shows a concentration of 0.5 %–1 %, reducing the angle of repose because the number of MgSt particles increases, which fills the porosity and the surface of the LG particles. In this condition, the surface of the LG particles becomes flat and smooth so that the particles above them move quickly and flow downwards to form a sloping cone. The number of particles is excessive at a concentration of 2 %–4 %, **creating** a layer on the surface of the LG particles. The many fines of MgSt particles inhibit the movement and flow of particles above them. The cone was sharp and the angle of repose was high.

3.5. Tap-Bulk

The Tap-Bulk values are shown in Table 2 and Fig. 4c. The waxy properties of the P-2HTCb particles on the surface of the LG facilitate the movement of LG to continuously fill the inter-particle porosity of the mixture, allowing the particles to achieve a stable arrangement. The higher the concentration of P-2HTCb, the Tap-Bulk value decreases because the P-2HTCb particles layer upon layer, allowing LG to achieve a stable arrangement quickly. Talc particles on the surface of the LG prevent humidity. A concentration of 1 % indicates the optimum free movement of LG enveloped by talc particles. Talc concentration decreases the Tap-Bulk value because LG moves between the tight talc particles. The cohesiveness between MgSt particles at the LG's surface separates when the mixture is subjected to repeated vertical mechanical forces, allowing the LG to move freely to fill the porosity of the mixture mass continuously. The concentration of MgSt increases, causing the Tap-Bulk value to increase. Cohesion between MgSt particles is released more, so the mixture of particles moves freely to reach the most stable arrangement.

The mixture mass of the P-2HTCb from a concentration of 0.5 %–4 % indicates a further decrease in the Tap-Bulk value because the P-2HTCb particle arrangement can fill the voids between the LG particles. As the concentration increases, the increase in P-2HTCb particles can still load the spaces between the LG particles even though the number decreases.

The mixture mass of the talc with a concentration of 0.5 % shows the dominance of the LG particle arrangement. At the same time, the talc particles have no effect because the number of particles is too small. In the talc mixture mass with a concentration of 1 %, the talc particles are on the surface of the LG particles. When the mixed mass receives mechanical movement, the talc particles move and fill the voids between the LG particles. The mixture mass of the talc with a concentration of 2 %–4 %, increasing the number of talc particles, can fill the voids between the LG particles so that the volume decrease is not too significant and the Tap-Bulk is small.

The mixture mass of the MgSt with a concentration of 0.5 %–4 % shows that increasing the MgSt concentration increases Tap-Bulk because MgSt has a low density, so the number of particles in the mixture mass is significant. Low density affects the measurement volume and alters the number of LG particles. The large number of MgSt fine particles causes a substantial decrease in volume, so the Tap-Bulk value becomes high.

3.6. Tablet weight

Table 3 shows the tablet weight for each experiment. This parameter was carried out to verify that each mixed mass could consistently flow to fill the die cavity of the tablet compression machine. The tablet mass in the die cavity is compressed into a tablet weighing around 700 mg with a slight deviation.

3.7. Hardness

Table 3 and Fig. 4d show each tablet's hardness value. The tablet hardness value indicates the deformation bond strength of the particles that make up the tablet. The type of glidant influences the tablet hardness profile with increasing glidant concentration. The tablet mass with P-2HTCb produced the highest tablet hardness compared to the other two glidants. The compressed mixture mass causes particle deformation. Furthermore, the compression pressure generates heat due to friction between particles. In addition, friction occurs between the particles and the metal punches and dies. P-2HTCb particles at the surface between the LG particles experience deformation and bond, thus bonding the deformation interlocking of the mixture mass particles and increasing tablet hardness. Tablet hardness at a talc concentration of 0.5 % is dominated by LG deformation interlocking. A 2 % talc concentration is the optimum concentration because it produces the highest tablet hardness. The deformation of the talc particles utilizes the absorbed humidity to bond the deformation interlocking of the mixture mass particles, resulting in high tablet hardness. At lower talc concentrations, the absorbed humidity is insufficient to bond the deformation interlocking of the mixture mass particles. At higher talc concentrations, the deformation of the humidity talc particles will stick together, resulting in lower tablet hardness. Tablet hardness at a 0.5 % MgSt concentration is influenced by the dominance of LG deformation interlocking, resulting in high hardness. At higher MgSt concentrations, the deformation of the MgSt particles containing saturated fat is insufficient to bond the deformation interlocking of the mixture mass particles, resulting in

Table 3
Evaluation values of tablets for weight, hardness, friability, and disintegration time.

Glidant	Concentration [%]	Weight [mg]	Hardness [kp]	Friability [%]	Disintegration time [min.]
Talc	**0.5**	701.30 ± 0.85	6.80 ± 0.80	0.86 ± 0.04	0.26 ± 0.05
	1.0	700.10 ± 1.45	5.90 ± 0.49	0.88 ± 0.01	0.14 ± 0.03
	2.0	700.90 ± 1.83	6.40 ± 0.36	0.91 ± 0.01	0.34 ± 0.03
	4.0	701.40 ± 0.78	5.50 ± 0.69	0.95 ± 0.02	0.46 ± 0.05
MgSt	**0.5**	701.00 ± 1.30	8.00 ± 0.78	0.85 ± 0.03	10.18 ± 0.05
	1.0	700.90 ± 1.64	5.80 ± 0.63	0.87 ± 0.02	9.23 ± 0.08
	2.0	701.80 ± 1.96	5.20 ± 0.51	0.93 ± 0.01	12.27 ± 0.09
	4.0	701.50 ± 1.76	7.30 ± 0.64	0.99 ± 0.01	14.89 ± 0.07
P-2HTCb	**0.5**	701.80 ± 1.21	7.90 ± 0.55	0.86 ± 0.06	1.21 ± 0.13
	1.0	700.50 ± 1.71	8.00 ± 0.39	0.82 ± 0.05	0.52 ± 0.10
	2.0	699.70 ± 1.23	8.10 ± 0.61	0.77 ± 0.03	1.27 ± 0.08
	4.0	702.00 ± 1.29	8.40 ± 0.53	0.70 ± 0.04	1.63 ± 0.07

Tablets with P-2HTCb glidant tended to have higher hardness and lower friability than the other two glidant tablets. The disintegration time with P-2HTCb glidant (<2 min) was slightly longer than that of tablets with talc glidant (<1 min) and significantly faster than that of tablets with MgSt glidant (9.23–14.89 min).

lower tablet hardness. At an MgSt concentration of 4 %, tablet hardness is influenced by the cohesiveness of the deformation of MgSt particles, so the tablet hardness is high.

Increasing the concentration of P-2HTCb increases tablet hardness. The P-2HTCb fines can fill particle porosity and porosity between LG particles. The arrangement of these particles shows a complementary composition so that the interlocking deformation becomes more stable when compressed.

The hardness of tablets with talc looks like a wave with peaks at concentrations of 0.5 % and 2 %. At a concentration of 0.5 %, tablet hardness was dominated by the interlocking of LG particle deformation, and talc fines did not affect the interlocking quality. Meanwhile, at a concentration of 2 %, the talc fines can fill the particles' porosity and the porosity between the LG particles so that this composition is stable when compressed into tablets. In tablets with a talc concentration of 1 %, small amounts of talc fines cause the tablet to have a lot of particle deformation porosity, so the tablet breaks easily when subjected to mechanical pressure. In tablets with a talc concentration of 4 %, there is too much fine talc, so the interlocking bonds between fine talc of deformation particles are not strong and break when mechanical pressure occurs.

The hardness of tablets with MgSt has a manger-like profile. In a tablet with an MgSt concentration of 0.5 %, tablet hardness influenced the dominance of interlocking deformation of LG particles. Deformation of MgSt fines does not affect the particle arrangement because the amount is small. Fines MgSt plays a more significant role in filling the LG particles' porosity so that the particles' surface is flat and smooth. When compressed, the particles form a compact deformation, strong interlocking, and hard tablets. This condition causes the hardness of tablets with a MgSt concentration of 0.5 % to be higher than that of tablets with 0.5 % talc. The hardness of tablets with MgSt concentrations of 1 % and 2 % showed a decrease. Fines MgSt at both concentrations filled the porosity of the LG particles, and the remainder filled the porosity between the LG particles. The higher the concentration, the more MgSt fines are contained in the porosity between the LG particles. This particle arrangement, when compressed, produces tablets with much porosity that easily crack when subjected to mechanical pressure. Tablets with a 4 % MgSt concentration have a composition mechanism similar to tablets of the other three concentrations. Tablets with a concentration of 4 % are harder than tablets with a MgSt concentration of 1 % and 2 % because of the interaction between MgSt fines on the tablet surface. This interactive force occurs due to the cohesive force of the MgSt fines, thus forming an overlapping, layered deformation structure, a hard tablet surface, and a shiny tablet.

3.8. Friability

Friability values for each glidant concentration are shown in Table 3 and Fig. 4e. Pharmaceutically good tablet friability is <1 % [36–39]. The friability profile of tablets with P-2HTCb is opposite to that of the other two glidants. The deformation of the P-2HTCb particles, which bond interlocking between deformation particles of the mixture mass when compressed into tablets, can be kept when subjected to repeated mechanical movements, so the tablets have low friability. The concentration of P-2HTCb increased, showing lower tablet friability. Tablets containing talc and MgSt showed that tablet friability increased as the concentration of talc or MgSt increased. The humidity of talc deformation particles cannot keep the bond between particle mass on the interlocking condition, so tablet friability is high when exposed to repeated mechanical movements. Tablet containing MgSt is similar to tablets containing talc, where the interlocking deformation of MgSt particles cannot be kept due to weakened cohesiveness. This condition occurs due to repeated mechanical movements, so the tablet friability is high.

Increasing the concentration of P-2HTCb reduces tablet friability. Tablet friability is synergistic with tablet hardness. P-2HTCb fines are in the porosity of LG and the porosity between LG particles. The higher the concentration of P-2HTCb in both porosities, the more compact the deformation of the LG particles and the harder the tablet. Friability occurs due to the release of LG particle fragments or P-2HTCb fines on the tablet's surface. The P-2HTCb fines on the tablet surface experience interlocking, making them more stable when subjected to mechanical movement and releasing fewer particles.

The release of talc particles (0.5 %) fragments dominated the friability of tablets because the deformation of LG particles dominated interlocking. The friability of tablets with a 1 % talc concentration was due to the release of LG particle fragments or talc fines. Particle fragments are released due to the large amount of porosity in the tablet, so deformation is not resistant to mechanical movement. Tablet friability of talc concentrations of 2 % and 4 % was due to the release of talc fines on the tablet's surface and which were not tightly interlocked and released when mechanical movement occurred. Increasing the concentration of talc causes the number and layer of deformation of talc fines on the tablet surface to increase, resulting in more release of talc fines when there is mechanical movement.

The friability of tablets with 0.5 % MgSt is due to the release of MgSt particle fragments due to the dominance of interlocking deformation of LG particles. The friability of tablets with talc concentrations of 1 % and 2 % is due to the release of LG particle fragments or MgSt fines. Particle fragments or fines are released, due to the large amount of porosity formed in the tablet, so the deformation becomes friable when mechanical movement occurs. Tablets with an MgSt concentration of 4 %

were friable due to MgSt fines on the tablet surface coming off. Even though there is a fine cohesive force of MgSt, the interaction can separate because the mechanical energy provided is stronger than the energy of the cohesive force.

3.9. Disintegration

Disintegration times for various glidants and concentrations are shown in Table 3 and Fig. 4f. All tablets in this experiment met the pharmaceutically acceptable disintegration time ≤15 min. The profiles of the three graphs show that the tablet disintegration time with P-2HTCb is close to the tablet disintegration time with talc. Tablets containing P-2HTCb disintegrate due to repulsion between P-2HTCb particles when wetted by the disintegration test medium. This repulsion occurs due to the waxy properties of P-2HTCb. A 1 % P-2HTCb concentration shows the fastest disintegration due to the optimum amount of P-2HTCb particle deformation, resulting in sufficient tablet porosity for penetration of the disintegration test medium. At lower concentrations, disintegration is affected by tablet hardness and penetration of the disintegration test medium through the LG porosity, requiring a longer time. At higher concentrations, the tablet porosity is tight due to many deformations of the P-2HTCb particles, resulting in slower penetration of the disintegration test medium.

The disintegration process of talc-containing tablets begins with the absorption of humidity by the deformation of the talc particles on the tablet surface, which results in the release of the talc particles from the tablet. This condition allows the disintegration medium to penetrate the tablet's porosity and experience disintegration. A talc concentration of 1 % demonstrated the fastest tablet disintegration due to the optimal amount of talc particle deformation, ensuring sufficient tablet porosity for penetration of the disintegration medium. At lower concentrations, tablet disintegration is more influenced by tablet hardness. The disintegration medium needs longer penetration times to penetrate the LG porosity on the tablet. At higher concentrations, tablet porosity is tighter due to the deformation of more talc particles, resulting in slower media penetration times during disintegration tests.

The hydrophobic properties of MgSt stems from the saturated fatty acid stearate. The deformation of MgSt particles on the tablet surface shields against the disintegration test medium. The deformed MgSt particles attract each other due to their cohesive nature during compression. The ability of the disintegration test medium to penetrate the porosity between the deformed MgSt particles influences the wetting of the tablet surface. Wetting of the tablet surface takes longer because MgSt is highly hydrophobic, resulting in a longer tablet disintegration time.

The curve profile of tablet disintegration time with P-2HTCb is similar to that of tablet disintegration time with talc and MgSt. The three graphs show that 1 % concentration is the optimum concentration for the fastest disintegration time because, in this condition, the number of glidant particles in the tablet is sufficient to provide a way for the disintegration medium to wet the surface and enter the tablet's core. The tablet disintegration time at a glidant concentration of 0.5 % is influenced by the tablet's porosity, which is the entry point for the disintegration medium. The tablet disintegration time at concentrations of 2 % and 4 % is influenced by the speed of wetting or penetration of the disintegration medium towards the glidant particles on the tablet surface. The higher the glidant concentration, the longer it takes to wet or penetrate the glidant particles on the tablet surface.

4. Statistic

The results of the ANOVA statistical test are shown in Table 4. The ANOVA test for glidant types indicates that there are significant differences ($F_{count} > F_{criteria}$; $P_{value} < \alpha_{0.05}$) between glidant types in the values of flow time, angle of repose, Tap-Bulk, hardness, and disintegration time. The particle shape of each glidant influences the particle arrangement of each glidant in the mixture mass and the porosity of the tablet. The type of glidant does not make a significant difference ($F_{count} < F_{criteria}$; $P_{value} > \alpha_{0.05}$) on friability because the three glidants are fines and cohesive, which tend to stay on the tablet surface and are easily separated when there is mechanical movement.

The ANOVA test for glidant concentration showed significant differences between concentrations ($F_{count} > F_{criteria}$; $P_{value} < \alpha_{0.05}$) in the values of flow time, angle of repose, hardness, friability, and disintegration time. Concentration affects the mass volume of the mixture, tablet thickness, and tablet porosity. Concentration did not provide a significant difference ($F_{count} < F_{criteria}$; $P_{value} > \alpha_{0.05}$) on Tap-Bulk. Even though the volume of each concentration is different, the difference between Tap and Bulk is similar.

5. Conclusion

The results of experiments with P-2HTCb at a concentration of 0.5–4.0 % as a glidant against LG show that the optimum concentration (2 %) improves the flow time and angle of repose of the mixture mass. Increasing the concentration of P-2HTCb causes the Tap-Bulk value of the mixture mass and tablet friability to decrease, but increases tablet hardness. The optimum concentration (1 %) provides the fastest disintegration time. Compared to the other two glidant materials, P-2HTCb produces minimal dust when mixed with LG material. The reduction in dust is an advantage of P-2HTCb for being more environmentally and health-friendly. P-2HTCb comes from natural Cb with a relatively higher bulk density than the other two glidant materials. The presence of 2HT can increase the bulk density of the combination product (P-2HTCb) to reduce dust during mixing. P-2HTCb can be recommended as an alternative glidant candidate in environmentally and health-friendly pharmaceutical formulations.

CRediT authorship contribution statement

Wuryanto Hadinugroho: Writing – original draft, Supervision, Methodology, Investigation, Formal analysis, Data curation, Conceptualization. **Stephanie Florencia Winarko:** Investigation, Formal analysis, Data curation. **Echa Imanuela Sinta:** Investigation, Formal analysis, Data curation. **Senny Yesery Esar:** Supervision, Methodology, Formal analysis. **Jefri Prasetyo:** Supervision, Methodology, Formal analysis.

Declaration of competing interest

The authors declare that they have no known competing financial interests or personal relationships that could have appeared to influence

Table 4
ANOVA of flow time, angle of repose, Tap-Bulk, hardness, friability, and disintegration time.

Glidant	Flow time	Angle of repose	Tap-Bulk	Hardness	Friability	Disintegration time	Criteria
Fcount	65.6111	10.5786	7.5806	79.0034	1.2014	1640.4846	F (3.0088)
P-value	1.00×10^{-11}	1.30×10^{-4}	9.80×10^{-4}	1.41×10^{-12}	0.33	6.86×10^{-28}	α (0.05)
Concentration							
Fcount	143.3571	177.2467	3.1287	461.7071	57.7262	84150.9414	F (3.4028)
P-value	$4.50 \times 10^{-1}4$	4.20×10^{-15}	6.20×10^{-2}	6.98×10^{-20}	6.75×10^{-10}	7.06×10^{-47}	α (0.05)

the work reported in this paper.

Acknowledgment

The authors would like to thank the Ministry of Higher Education, Science, and Technology of the Government of Indonesia for providing financial assistance (613/WM01.5/N/2025). The authors would like to thank the laboratory facilities of the Faculty of Pharmacy, Widya Mandala Surabaya Catholic University.

References

[1] W. Hadinugroho, S. Martodihardjo, A. Fudholi, S. Riyanto, Esterification of citric acid with locust bean gum, Heliyon 5 (2019) e02337, https://doi.org/10.1016/j.heliyon.2019.e02337.
[2] W. Hadinugroho, S. Martodihardjo, A. Fudholi, S. Riyanto, Preparation of citric acid-locust bean gum (CA-LBG) for the disintegrating agent of tablet dosage forms, J. Pharm. Innov. 17 (2022) 1160–1175, https://doi.org/10.1007/s12247-021-09591-0.
[3] W. Hadinugroho, S. Martodihardjo, A. Fudholi, S. Riyanto, J. Prasetyo, Hydroxypropyl methylcellulose as hydrogel matrix and citric acid-locust bean gum as negative matrix for controlled release tablet, ACS Omega 0 (2023), https://doi.org/10.1021/acsomega.2c07432.
[4] A. Awad, S.J. Trenfield, A.W. Basit, Solid oral dosage forms, in: A. Adeboye (Ed.), Remingt. Sci. Pract. Pharm., thirteenth ed., Elsevier Inc., Philadelphia, 2020, pp. 333–3358, https://doi.org/10.1016/C2018-0-04991-9.
[5] P. Zarmpi, T. Flanagan, E. Meehan, J. Mann, N. Fotaki, Impact of magnesium stearate presence and variability on drug apparent solubility based on drug physicochemical properties, AAPS J. 22 (2020), https://doi.org/10.1208/s12248-020-00449-w.
[6] P.J. Sheskey, C.G. Walter, C.G. Cable, Handbook of Pharmaceutical Excipients, eighth ed., Pharmaceutical Press and American Pharmacists Association, London-Washington DC, 2017.
[7] Y. Meng, W. Xie, H. Wu, S.M. Tariq, H. Yang, Evolution of black talc upon thermal treatment, Minerals 12 (2022) 1–14, https://doi.org/10.3390/min12020155.
[8] J.A. Bazar, M. Rahimi, S. Fathinia, M. Jafari, V. Chipakwe, S.C. Chelgani, Talc flotation - an overview, 8–13, https://doi.org/10.3390/min11070662, 2021.
[9] A. Fajdek-Bieda, A. Wróblewska, The use of natural minerals as reinforcements in mineral-reinforced polymers: a review of current developments and prospects, Polymers 16 (2024), https://doi.org/10.3390/polym16172505.
[10] C.A. Hobbs, K. Saigo, M. Koyanagi, S. mo Hayashi, Magnesium stearate, a widely-used food additive, exhibits a lack of in vitro and in vivo genotoxic potential, Toxicol. Rep. 4 (2017) 554–559, https://doi.org/10.1016/j.toxrep.2017.10.003.
[11] S.P. Delaney, M.J. Nethercott, C.J. Mays, N.T. Winquist, D. Arthur, J.L. Calahan, M. Sethi, D.S. Pardue, J. Kim, G. Amidon, E.J. Munson, Characterization of synthesized and commercial forms of magnesium stearate using differential scanning calorimetry, thermogravimetric analysis, powder X-ray diffraction, and solid-state NMR spectroscopy, J. Pharm. Sci. 106 (2017) 338–347, https://doi.org/10.1016/j.xphs.2016.10.004.
[12] N. Veronica, P.W.S. Heng, C.V. Liew, Magnesium stearate fatty acid composition, lubrication performance and tablet properties, AAPS PharmSciTech 25 (2024) 1–15, https://doi.org/10.1208/s12249-024-02980-x.
[13] O.M. Ajayi, S. Amin, Flow and performance effects of talc alternatives on powder cosmetic formulations, Int. J. Cosmet. Sci. 43 (2021) 588–600, https://doi.org/10.1111/ics.12733.
[14] P. Hiremath, K. Nuguru, V. Agrahari, Material Attributes and Their Impact on Wet Granulation Process Performance, Elsevier Inc., 2018, https://doi.org/10.1016/B978-0-12-810460-6.00012-9.
[15] R. Nasrin, M.A. Gafur, A.H. Bhuiyan, Characterization of isotactic polypropylene/talc composites prepared by extrusion cum compression molding technique, Mater. Sci. Appl. 6 (2015) 925–934, https://doi.org/10.4236/msa.2015.611093.
[16] S. Tanpong, A. Cherdthong, B. Tengjaroenkul, U. Tengjaroenkul, S. Wongtangtintharn, Evaluation of physical and chemical properties of citric acid industrial waste, Trop. Anim. Health Prod. 51 (2019) 2167–2174, https://doi.org/10.1007/s11250-019-01917-y.
[17] D.P. Dahiya, R. Kumar, R. Malviya, Purification and characterization of Natural Polymer locust bean gum. , 2023, https://doi.org/10.37896/jxu16.10/021.
[18] M. Oryzas, S. Wongtangtintharn, B. Tengjaroenkul, A. Cherdthong, S. Tanpong, P. Bunchalee, P. Pootthachaya, A. Reungsang, S. Polyorach, Physico-chemical characteristics and amino acid content evaluation of citric acid by-product produced by microbial fermentation as a potential use in animal feed, Fermentation 7 (2021), https://doi.org/10.3390/fermentation7030149.
[19] W. Hadinugroho, S.F. Winarko, E.I. Sinta, S.Y. Esar, J. Prasetyo, Effect of heating temperature on citric acid-locust bean gum synthesis, Pharm. Educ. 24 (2024) 216–221, https://doi.org/10.46542/pe.2024.243.216221.
[20] S.Y. Singh, Salwa, R.K. Shirodkar, R. Verma, L. Kumar, Enhancement in dissolution rate of atorvastatin trihydrate calcium by formulating its porous tablet using sublimation technique, J. Pharm. Innov. 15 (2020) 498–520, https://doi.org/10.1007/s12247-019-09397-1.
[21] W. Hadinugroho, K. Foe, Y. Tjahjono, C. Caroline, S. Yesery Esar, H. Wijaya, M. Annabella Jessica, Tablet formulation of 2-((3-(Chloromethyl)benzoyl)oxy) benzoic acid by linear and quadratic models, ACS Omega 7 (2022) 34045–34053, https://doi.org/10.1021/acsomega.2c03147.
[22] The United States Pharmacopeial Convention, Pharmacopeia 41-National Formulary, 36, 41st ed., Twinbrook Parkway, Rockville, 2018.
[23] M.E. Aulton, K.M.G. Taylor, Aulton's Pharmaceutics the Design and Manufacture of Medicines, Churchill Livingstone Elsevier, New York, 2017.
[24] R.S. Singh, N. Kaur, V. Rana, R.K. Singla, N. Kang, G. Kaur, H. Kaur, J.F. Kennedy, Carbamoylethyl locust bean gum: synthesis, characterization and evaluation of its film forming potential, Int. J. Biol. Macromol. 149 (2020) 348–358, https://doi.org/10.1016/j.ijbiomac.2020.01.261.
[25] P. Duan, B. Zhi, L. Coburn, C.L. Haynes, K. Schmidt-Rohr, A molecular fluorophore in citric acid/ethylenediamine carbon dots identified and quantified by multinuclear solid-state nuclear magnetic resonance, Magn. Reson. Chem. 58 (2020) 1130–1138, https://doi.org/10.1002/mrc.4985.
[26] S. Gillet, M. Aguedo, C. Blecker, N. Jacquet, A. Richel, Use of 13C-NMR in structural elucidation of polysaccharides: case of locust bean gum, Liège. , 2014.
[27] A. Idström, S. Schantz, J. Sundberg, B.F. Chmelka, P. Gatenholm, L. Nordstierna, 13C NMR assignments of regenerated cellulose from solid-state 2D NMR spectroscopy, Carbohydr. Polym. 151 (2016) 480–487, https://doi.org/10.1016/j.carbpol.2016.05.107.
[28] D. Tian, Y. Qiao, Q. Peng, Y. Zhang, Y. Gong, L. Shi, X. Xiong, M. He, X. Xu, B. Shi, A poly-D-mannose synthesized by a one-pot method exhibits anti-biofilm, antioxidant, and anti-inflammatory properties in vitro, Antioxidants 12 (2023) 1–21, https://doi.org/10.3390/antiox12081579.
[29] I. Trabelsi, S. Ben Slima, N. Ktari, M. Bouaziz, R. Ben Salah, Structure analysis and antioxidant activity of a novel polysaccharide from Katan seeds, BioMed Res. Int. 2021 (2021), https://doi.org/10.1155/2021/6349019.
[30] R. Amelia, M.U. Beandrade, W.N. Hasmar, Formulation and physical characterization of black soybean (Glycine max L.) variety of detam II tablets with dry granulation method, Int. J. Nat. Sci. Eng. 5 (2021) 30–38, https://doi.org/10.23887/ijnse.v5i1.33441.
[31] S. Wati, D. Saryanti, Effervescent granule formulation of bitter melon extract (Momordica charantia L .) with gelatin as A wet granulation binder, J. Nutraceuticals Herb. Med. 2 (2019) 20–28.
[32] A.T. Pradana, C. Steffany, R. Yulia, Formulation and stability study of detam I soybean variety (Glycine max (L.) Merr.) effervescent granules with different type of effervescent agents, Acta Pharm. Indones. 46 (2021) 38–43, https://doi.org/10.5614/api.v46i2.15751.
[33] N.S.F. Putri, The the effect of uncontrolled addition of gelatin in paracetamol tablet formulation and the evaluation, J. Sci. Technol. Res. Pharm. 2 (2023) 31–37, https://doi.org/10.15294/jstrp.v2i1.57436.
[34] J. Clayton, An Introduction to Powder Characterization, Elsevier Inc., 2018, https://doi.org/10.1016/B978-0-12-810460-6.00021-X.
[35] H.M. Beakawi Al-Hashemi, O.S. Baghabra Al-Amoudi, A review on the angle of repose of granular materials, Powder Technol. 330 (2018) 397–417, https://doi.org/10.1016/j.powtec.2018.02.003.
[36] D. Sharma, M. Singh, D. Kumar, G. Singh, M.S. Rathore, Formulation development and evaluation of fast disintegrating tablets of Ambroxol hydrochloride for pediatrics- a novel approach for drug delivery, Indian J. Pharm. Educ. Res. 48 (2014) 40–48, https://doi.org/10.5530/ijper.48.4s.6.
[37] T.L. Chee, F.A.A. Majid, M.C. Iqbal, Development of Diabecine^{TM} tablet and confirmation of its physical properties and pharmaceutical safety analysis, Sains Malays. 46 (2017) 597–604, https://doi.org/10.17576/jsm-2017-4604-12.
[38] S.A. Fouad, F.A. Malaak, M.A. El-Nabarawi, K.A. Zeid, Development of orally disintegrating tablets containing solid dispersion of a poorly soluble drug for enhanced dissolution: in-vitro optimization/in-vivo evaluation, PLoS One 15 (2020) 1–17, https://doi.org/10.1371/journal.pone.0244646.
[39] A. Aslani, M. Beigi, Design, formulation, and physicochemical evaluation of montelukast orally disintegrating tablet, Int. J. Prev. Med. 7 (2016), https://doi.org/10.4103/2008-7802.193097.